# Alternation in the Gap-junctional Intercellular Communication Capacity during the Maturation of Osteocytes in the Embryonic Chick Calvaria

Ziyi Wang, Naoya Odagaki, Tomoyo Tanaka, Mana Hashimoto, Masahiro Nakamura, Satoru Hayano, Yoshihito Ishihara, Noriaki Kawanabe, Hiroshi Kamioka

Department of Orthodontics, Okayama University Graduate School of Medicine, Dentistry, and Pharmaceutical Sciences, Okayama, Japan

OKAYAMA UNIV.

## Introduction

To further understand the mechanism of bone development, it is therefore important to quantify the difference in Gap-Junctional Intercellular Communication (GJIC) capacity between young and developmentally mature osteocytes. For this aim, we established an embryonic chick calvaria growth model, which reflected the growth of the calvaria in embryos at 13 to 21 days of age. This model can also reveal the relationship between the osteocyte location and its age. So this model actually quantified and confirmed our previous finding that different aged osteocytes have different morphologies, with the young osteocytes having a more spherical shape and developmentally mature osteocytes being more spindle shaped. Next, the FRAP technique was applied to calculate the dye displacement ratio in cell bodies and permeability in the cellular process network. In addition, a comparison was made between the young and developmentally mature osteocytes.

## Materials and Methods

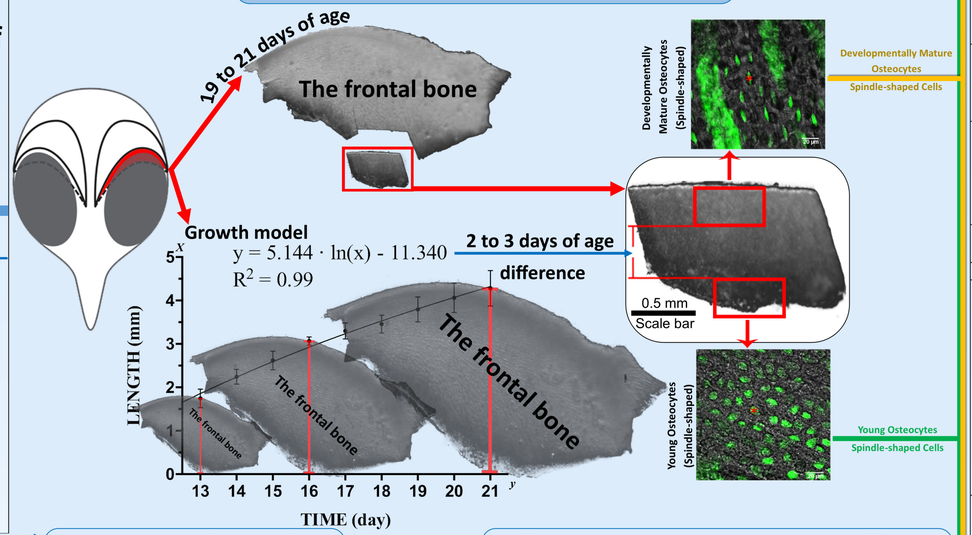


The estimated age in the regions of young and developmentally mature osteocytes

| Age (days) | Estimated age in young region 100-450 μm (day) | Estimated age in developmentally mature region 850-1,300 μm (day) | Age difference (day) |
|---|---|---|---|
| 19 | 0.35 - 1.57 | 2.93 - 4.28 | 2.58 - 2.70 |
| 20 | 0.36 - 1.65 | 3.00 - 4.50 | 2.72 - 2.85 |
| 21 | 0.50 - 1.85 | 3.34 - 4.82 | 2.84 - 2.97 |
| Mean | 1.05 | 3.82 | 2.78 |

The morphometric data of the differently shaped osteocytes

| | Young osteocytes (n=47) | Developmentally mature osteocytes (n=25) |
|---|---|---|
| Shortest diameter (μm) [b] | 6.14 + 1.01 | 4.50 + 0.99**** |
| Longest diameter (μm) [a] | 10.48 ± 1.32 | 12.90 ± 2.50*** |
| Diameter ratio, long/short [c] | 1.75 + 0.34 | 2.91 + 0.46**** |
| Cell volume (μm³) [b] | 197.70 ± 70.98 | 154.90 ± 78.51* |
| Cell surface area (μm²) [b] | 196.60 + 47.01 | 179.70 + 62.72 $^{P>0.09}$ |
| | from neighbour-target cells couple (n=243) | from neighbour-target cells couple (n=101) |
| Cell-cell distance, mass center (μm) [a] | 16.04 ± 3.91 | 16.30 ± 6.04 $^{P>0.95}$ |
| Boundary-boundary shortest length (μm | 6.42 ± 2.87 | 7.70 ± 3.59** |
| | from phalloidin-stained samples (n=10) | from phalloidin-stained samples (n=10) |
| Number of processes [b] | 50.40 ± 4.5 | 50.40 ± 6.20 $^{P>0.99}$ |
| Number of contributing processes [b] | 17.40 + 2.59 | 17.10 + 3.90 $^{P>0.84}$ |

The values show the mean ± SD
a: Welch's *t*-test; b: Student's *t*-test; c: Mann-Whitney *U* test

A schematic illustration of the laser pathway and a 3D reconstructed image.

**(A)** The schematic illustration shows that the processes above and below the target osteocyte also lay within the laser path.
**(B)** A 3D reconstructed image shows bone cells stained with Texas red-X phalloidin (red).
**(C)** A prebleaching image which was used to count the total number of processes.
**(D)** A postbleaching image of the same target cell as (A) and (B), which was used for 3D superimposition.
**(E)** A 3D superimposition image which was used to count the number of contributing processes. The green part comes from the prebleaching image, the red part comes from the post-bleaching image. (The white asterisks represent the target osteocyte, scale bar = 3um)

### Counting the number of cell processes contributing to dye transport

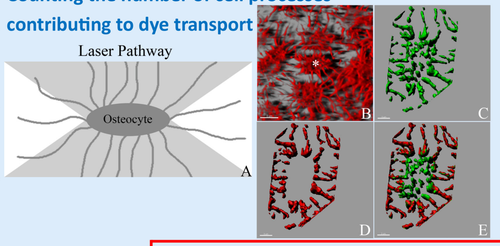


### Mathematic model of simple diffusion

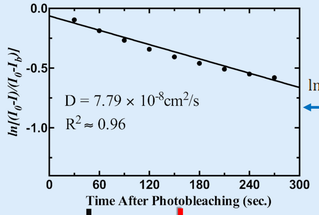


$$\ln\left(\frac{I_0 - I_{(t')}}{I_0 - I_b}\right) = -\frac{V_r t' D}{d^2}$$

In all valid data

### Fluorescence recovery after photobleaching (FRAP)

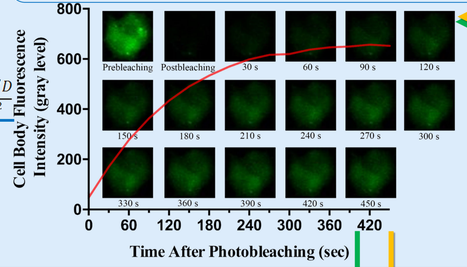


$R^2 < 0.96$ Non-Fitted

$R^2 \geq 0.96$ Fitted

### hypothesis for fitted and non-fitted model cells

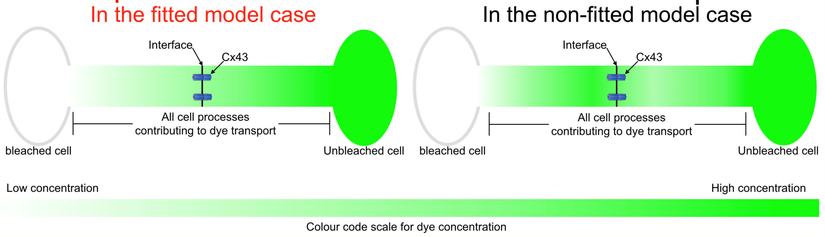


This model also can therefore be used to identify the simple diffusion GJIC pattern cells (fitted model) and the accelerated diffusion GJIC pattern cells (non-fitted model).

## Results

* *P*<0.05, ** *P*<0.01, *** *P*<0.001, **** *P*<0.0001

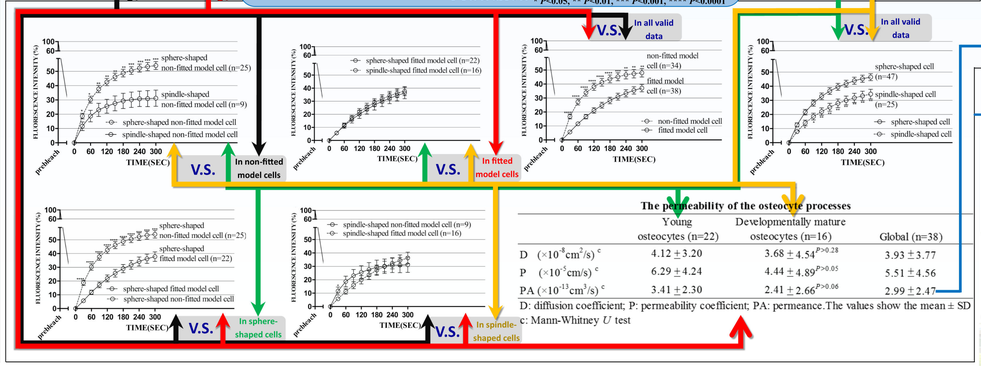


The permeability of the osteocyte processes

| | Young osteocytes (n=22) | Developmentally mature osteocytes (n=16) | Global (n=38) |
|---|---|---|---|
| D (×10⁻⁸cm²/s) [c] | 4.12 ± 3.20 | 3.68 ± 4.54 $^{P>0.28}$ | 3.93 ± 3.77 |
| P (×10⁻⁵cm/s) [c] | 6.29 ± 4.24 | 4.44 ± 4.89 $^{P>0.05}$ | 5.51 ± 4.56 |
| PA (×10⁻¹³cm³/s) [c] | 3.41 ± 2.30 | 2.41 ± 2.66 $^{P>0.06}$ | 2.99 ± 2.47 |

D: diffusion coefficient; P: permeability coefficient; PA: permeance. The values show the mean ± SD
c: Mann-Whitney *U* test

### The number of opened Cx43 channels in each cell

Please notice that the mathematic model for calculating the permeability is based on a simple diffusion procedure and assumes that the tracer moves evenly in processes. This means that in all of the fitted model cells, the speed of tracer through the interface between two processes was the same as the tracer movement in the cell process channels. So we can assume that the *PA* of the processes was equal to the *PA* of interface. The combined relationship is shown in the formula below:

$$PA_{interface} = N_{pore} \times PA_{pore}$$

Where $N_{pore}$ is the number of open channels on the interface between two processes; $PA_{interface}$ is equal to the process permeability; and $PA_{pore}$ indicates the single gap junction channel permeability. Based on the above equation, the number of open Cx43 channels in interface can be calculated. The combination of young and old fitted model cells was **149.4**; this sums up all of the contributing processes.

## Conclusions

1. GJIC was decreased during the developmental maturation of osteocytes.
2. GJIC between osteocytes could be regulated and almost half of the gap junction channels have the same permeability as the cell processes for Calcein transfer.
3. Indirect evidence of the active transduction of molecules through the Cx43 channel.

OKAYAMA UNIV.

**Acknowledgements**

**This work was partially supported by the Japan Society for Promotion of Science KAKENHI Grant Number JP16H05549.**